A study of the sprays formed by impinging jets in laminar and turbulent flow

By N. DOMBROWSKI AND P. C. HOOPER

High Speed Fluid Kinetics Laboratory, Department of Chemical Engineering, Imperial College, London, S.W. 7

(Received 9 April 1963 and in revised form 5 September 1963)

A study has been made of the factors influencing the break-down of sheets formed by the impingement of two liquid jets. It is shown that disintegration generally results from the formation of unstable waves of aerodynamic or hydrodynamic origin. While the characteristics of the former waves are fairly well understood, little is known about the latter. The results of this study indicate that hydrodynamic (or 'impact') waves are generated when the Weber number of each jet ($\rho_l D V^2 \sin^2\theta/\gamma$, where ρ_l is the liquid density, D the jet diameter, V the mean jet velocity, θ the half-angle of impingement, and γ is the surface tension) is above a critical value, and that their formation is independent of the Reynolds number. Drop sizes have been measured and are shown to be critically dependent upon the mechanism of disintegration.

Introduction

When two jets of liquid are caused to impinge, a flat sheet is produced in a plane perpendicular to that containing them. It has been found (Heidman, Priem & Humphrey 1957; Tanasawa, Sasaki & Nagai 1957) that the sheet breaks down through one or other of two principal mechanisms. First, a relatively unruffled sheet may be produced which eventually breaks down through the super-imposition of aerodynamic waves. Secondly, waves are produced at the point of impingement. These waves control the breakdown of the sheet over a wide range of ambient air densities, particularly below atmospheric (Dombrowski & Hooper 1962). Stehling (1952) and Dombrowski & Hooper have shown that these latter waves persist *in vacuo* (28 in. Mercury vacuum) and have concluded that they were not caused by aerodynamic reaction but resulted from the impact of the two jets. Heidman *et al.* considered the mechanism of disintegration to be a function of jet velocity while Tanasawa *et al.* related the mechanism to the Reynolds number of the individual jets.

The principle object of this research has been to clarify the problem, and to this end, a pair of impinging water jets were employed which could be maintained in either laminar or turbulent flow over a wide range of velocities (corresponding to a range of Reynolds numbers up to 12,000).

It is concluded that both the mechanism of disintegration of a sheet produced by impinging jets, and the resulting drop size are principally dependent upon the velocity profiles across the jets, and their angles of impingement.

Experimental

Rupe (1953) has shown that in order to obtain fully developed velocity profiles it is necessary to pass the liquid through very long tubes (length/diameter = $L/D = 400$). Heidman *et al.* have shown that jet diameter has little effect on the spray, and this dimension has, therefore, been kept constant in the present work. Precision-bore glass tubes, 20 cm long and 0·05 cm internal diameter, were used to produce the jets, the entry to each tube being flared by heating the glass and

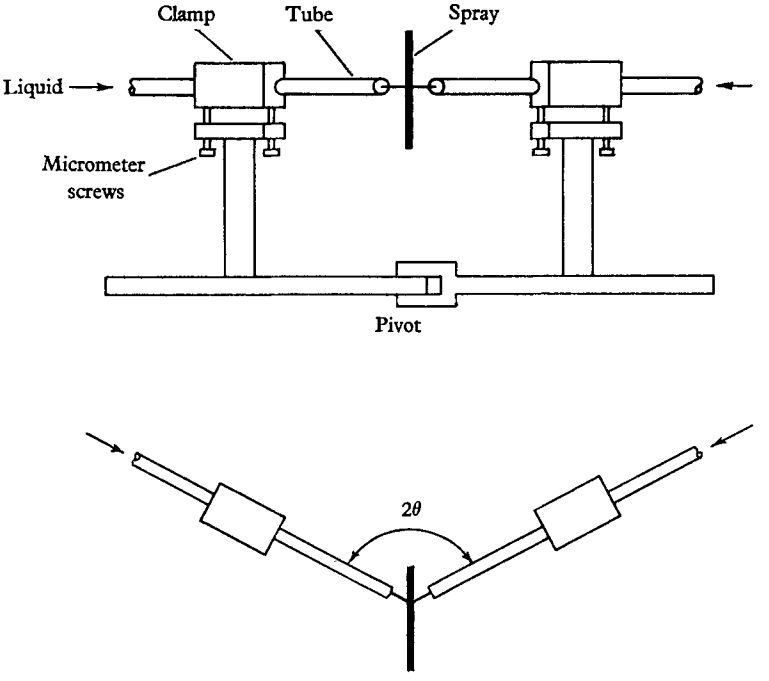

FIGURE 2. Tube holder.

inserting a conical tool. Each tube was connected to a surge chamber similar to that designed by Rupe so that laminar jets could be produced over a range of Reynolds numbers up to 12,000. Laminar flow was confirmed from measurements of the pressure drop along the tubes (Hooper 1959). The jets were made turbulent by inserting wires into the flared entry of each tube. Typical examples of laminar and turbulent jets are shown in figure 1, plate 1.

Liquid was fed to each tube from a storage vessel by compressed air, the flow rate being measured by a rotameter. The apparatus used for positioning the two tubes is shown diagrammatically in figure 2. It consists essentially of two clamps, each of which can be pivoted to give a maximum angle of 140° and be individually adjusted by means of micrometer screws. Heidman *et al.* have also shown that the free jet length has little effect on the appearance of the spray provided that no break-up of the jets has occurred. Consequently in the present work the jet length has also been kept constant, a value of 0·2 cm being chosen since this is well within the break-up lengths of the turbulent and laminar jets studied in this research.

Tests were carried out with a pair of laminar jets and with a pair of turbulent jets. In each case water containing 0·5 % Nigrosine dye was employed and the jets were caused to impinge at angles (2θ) of 50, 80, 110 and 140° at mean velocities† (V) of 730, 1160, 1600 and 1950 cm/sec. A microsecond flash photograph, and an 8000 frame per second high-speed ciné-film were taken for every experiment. Drop sizes were measured from the flash photographs while the ciné-films were used to determine the sheet velocities by measuring the distances moved by surface irregularities and waves.

Results

Mechanisms of disintegration

Figure 3, plates 2 and 3, shows a selection of photographs obtained for the pair of impinging turbulent jets. The photographs demonstrate that under all operating conditions waves are produced at the point of impact and that except at the lowest angle and velocity (50°, 730 cm/sec) these waves cause the sheet to disintegrate into bands of drops, particularly at the higher jet velocities. At low angles of impingement much of the liquid is concentrated on the axis. At higher angles the liquid becomes more uniformly dispersed.

Figure 4, plates 4 and 5, shows a selection of photographs obtained for the pair of laminar jets and demonstrates that in this case the mechanism of disintegration is affected both by the angle of impingement and by the jet velocity. The photographs indicate a tendency for instability to be more pronounced near the axis of the sheet. At low velocities this sector widens and becomes more stable as the angle of impingement is increased. Thus, at a velocity of 730 cm/sec and an angle of 140° a completely unruffled sheet is produced bounded by thick rims. Under these conditions drops are produced directly from the rims.

At higher velocities the sheet can be divided into three principal regions, the magnitude of each varying with jet velocity and angle of impingement. In the central sector, below the point of impact, disintegration occurs earlier than in the rest of the sheet by means of waves similar to those observed for turbulent jets (e.g. 110°, 1950 cm/sec). The second region lies adjacent to the central zone and appears to be relatively smooth. It extends further from the point of impact and disintegrates by aerodynamic wave motion. The photographs also show stable high-frequency circumferential waves superimposed on the sheet. It is not clear whether these waves are caused by the jet impact or whether they have a mechanical origin in the equipment. The third region extends above the origin and its characteristics depend upon the operating conditions. At an angle of 50° a thick unbroken rim is produced very close to the point of impact. As the angle is further increased, particularly at the higher jet velocities (e.g. 110°, 1950 cm/sec) the upper region disintegrates by aerodynamic waves; at the highest angles and velocities impact waves predominate over the whole sheet.

At intermediate velocities (1160 cm/sec, 110°, 140°) the waves appearing in the central sector are rapidly damped and the breakdown of the sheet appears to be controlled by radial streaks emanating from the point of impact. Figure 5, plate 6, shows an enlargement of part of a sheet (1160 cm/sec, 110°). It can be

† Mean velocity = flow rate/cross-sectional area of tube.

seen that the streaks interact with the circumferential waves to form small ridges. Since the liquid contains dye, large ridges appear as black dots. Some of the ridges appear indistinct. This is probably due to the fact that they occur on the farther side of the sheet and are therefore viewed through it. Sir Geoffrey Taylor (private communication) has suggested that these streaks occur as a result of some turbulence in the jet which is pulled out into long eddies in the rapidly straining part of the fluid where the two jets meet.

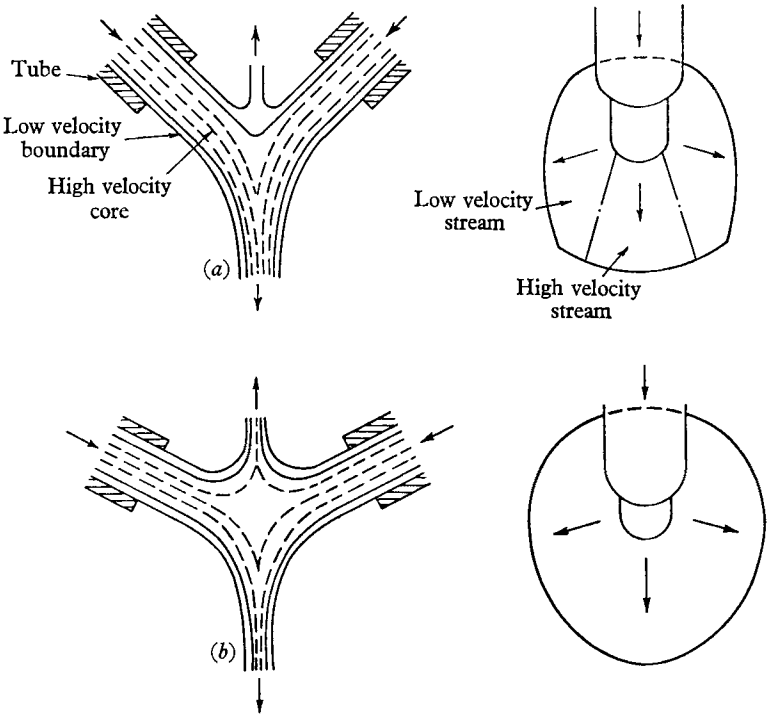

FIGURE 6. Impingement of two laminar jets.

Comparison of the photographs in figures 3 and 4 indicates that the mechanism of sheet disintegration is independent of Reynolds number and is affected only by the velocity profile across the jet and the angle of impingement. It is reasonable to assume that the onset of 'impact-wave' instability is related to the inertial force of the jets, and will thus, for a low viscosity liquid, be determined by a critical Weber number. On this basis, the differences between 'laminar' and 'turbulent' impact may be explained qualitatively as follows.

When laminar flow is fully established in a tube a parabolic velocity profile is set up wherein the axial velocity is twice the mean velocity. This profile will tend to persist in the free jet leaving the tube. The impingement of laminar jets can then be represented diagrammatically as shown in figure 6 where each jet is assumed to consist of a high velocity core surrounded by an annulus of slower moving liquid. At low angles of impingement (figure 6 (*a*)), a high velocity stream moves downstream while the coalescing low velocity annuli form low-velocity liquid laminae adjacent to it. Thus on the assumption that a high inertial force causes instability, we can expect that the high-velocity stream concen-

trated around the sheet axis will disintegrate through 'impact' waves while the rest of the sheet, depending upon the resulting velocity, will either extend to a region of equilibrium or will disintegrate through aerodynamic waves. At larger angles of impingement (figure 6 (*b*)) and particularly at high jet velocities the high velocity stream is more evenly distributed, and 'impact-wave' disintegration predominates over the major part of the sheet.

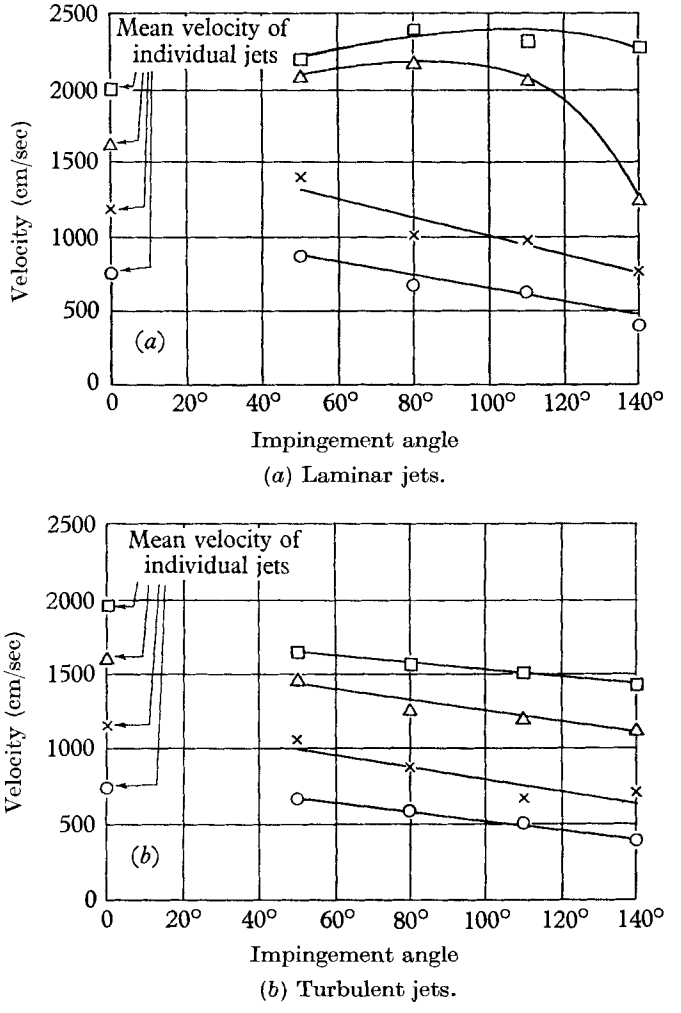

FIGURE 7. Variation of sheet velocity with impingent angle.

It can be expected at lower jet velocities that the core will become less dominant and that the low velocity annulus will tend to control the stability of the sheet to a greater extent. This is indicated at 1160 cm/sec where impact waves persist only for a short time, and at 730 cm/sec, particularly at the higher angles of impingement, where a completely unruffled sheet is formed.

When turbulent flow is fully established in a tube the velocity profile is effectively flat, secondary effects caused by low-velocity boundaries are thus

non-existent and consequently, for Weber numbers greater than the critical, impact waves predominate over the whole range of operating conditions.

Some confirmation of the above hypothesis can be adduced from the curves in figure 7 which show that for laminar jets the central regions of the resultant sheets tend to move at a higher velocity than the sheets produced by turbulent jets, and that at low angles of impingement where impact losses are at a minimum the velocity is higher than the mean velocity of the jets.

If the Weber number is defined by $\rho_l D V^2 \sin^2\theta/\gamma$, where ρ_l is the liquid density, D the tube diameter, V the mean jet velocity, θ the half-angle of impingement, and γ is the surface tension, then the results† for the turbulent jets indicate that the critical value of the Weber number, above which impact waves are produced, lies between 66 and 165. This may be compared with the range of 84–126 calculated from the results of Heidman *et al.* Taylor (1960) has studied the impingement of laminar jets with flat velocity profiles and found that aerodynamic waves only were produced with 0·227 cm diameter jets impinging at an angle of 60° at a head of 155 cm water. The jets were produced from sharp-edged orifices and caused to impinge downstream of the vena-contracta. The jet diameters at impingement were not recorded and it is thus not possible to accurately calculate the appropriate Weber number. However, approximate measurements made from Taylor's photographs indicate that undisturbed sheets were produced with a Weber number of 134 at an orifice Reynolds number of 6900.

Mean drop size

Drop sizes, expressed as surface-volume mean diameters d_s ($= \Sigma nd^3/\Sigma nd^2$, where n is the number of drops of diameter lying within a small size range about d) were measured in the central region of the sprays to show the relative effect of impingement angle and jet velocity.

(*a*) *Turbulent jets.* Figure 8(*a*) shows the variation of mean drop size with jet velocity at various angles of impingement. The curves show a consistent decrease of drop size with increasing angle and velocity and the results have been correlated with the variables to give

$$d_s = 4/V^{0\cdot79}\sin^{1\cdot16}\theta.\ddagger \tag{1}$$

Equation (1) is plotted in figure 9.

It will be noted that V and $\sin\theta$ are raised to different powers. This is not surprising since it would be expected that θ controls drop size in two ways—first in its effect on the component of velocity of the two jets towards each other (i.e. $V\sin\theta$), and secondly in its effect on sheet thickness.

On the other hand, Fry, Thomas & Smart (1954) studying the impingement of $\frac{1}{16}$ in. diameter jets ($L/D \approx 20$) found that the mass median diameter, d_m, is given by

$$d_m = 0\cdot775 - 0\cdot000164\, V\sin\theta, \tag{2}$$

where it is seen that the two variables have the same indices.

† The following comparisons are for jets of water so that V and θ are the only variables.

‡ The symbols in all equations are in c.g.s. units.

Tanasawa *et al.* found for head-on impingement ($2\theta = 180°$) with a range of tube diameters from 0·04 to 0·1 cm and of unspecified tube lengths that

$$d_s = 1{\cdot}73 \frac{D^{0{\cdot}75}}{V^{0{\cdot}5}} \left(\frac{\gamma}{\rho_l}\right)^{0{\cdot}25}, \tag{3}$$

where D is the tube diameter (cm), γ is the surface tension (dyn/cm) and ρ_l is the liquid density (g/c.c.), while Dombrowski & Hooper found, for an impinging jet nozzle consisting of a pair of 0·053 cm diameter convergent-divergent tubes impinging at 110° ($L/D \approx 2$), that

$$d_s = 0{\cdot}0231\, \gamma^{0{\cdot}16} / V^{0{\cdot}32} \rho_l^{0{\cdot}06} \rho_a^{0{\cdot}1}, \tag{4}$$

where ρ_a is the air density (0·0012 to 0·01 g/c.c.).

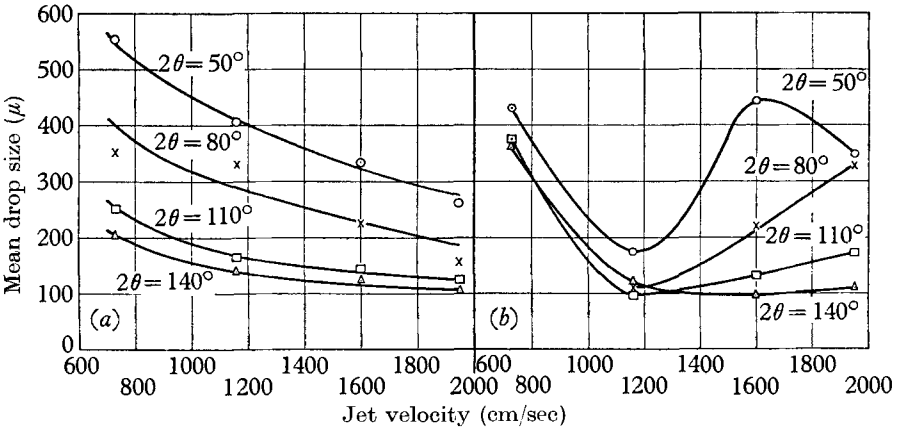

FIGURE 8. Variation of drop size with jet velocity. (*a*) Turbulent jets; (*b*) laminar jets.

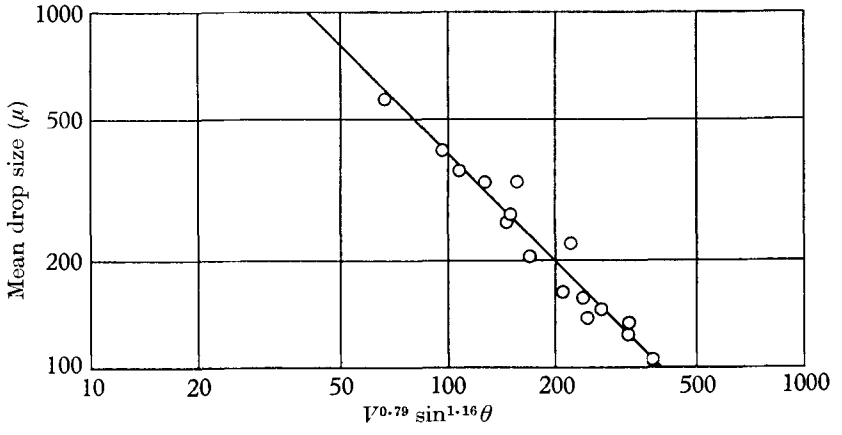

FIGURE 9. Correlation of drop-size results for impingement of turbulent jets.

It can be assumed that turbulent jets were employed in the previous investigations since no attempts were made to produce laminar flow. There is insufficient evidence to explain fully the differences between the above equations but the reason is likely to be due to the different velocity profiles occurring in the jets as a result of the varying L/D ratios employed in each of the investigations.

(*b*) *Laminar jets.* The corresponding drop-size results for laminar jet impingement are given in figure 8(*b*). The curves show that contrary to the results for turbulent jets the drop size initially decreases rapidly as the velocity is raised from 730 to 1160 cm/sec, and then increases with further increase of velocity to an extent depending upon the angle of impingement. At an angle of 50° the drop size rises to a maximum value at 1600 cm/sec after which it diminishes.

These results can be explained by consideration of the basic process of drop formation from diverging sheets (Dombrowski & Fraser 1954) which consist principally of the tearing away of wavelengths or half-wavelengths of the sheet, their rapid coalescence into ligaments and the final break-down into drops; in the absence of any internal or external flow disturbance, the leading edge of the sheet attains a region of equilibrium whereby a stationary rim is formed from which drops are produced. Sheets produced by turbulent jet impingement disintegrate through wave motion for practically the whole range of operating conditions although it is not clear from the photographs how the sheet fragments are related to the waves on the coherent sheet. For a given liquid-gas system aerodynamic reaction gives rise to exponentially growing waves whose amplitude and wavelength are related solely to the relative liquid-gas velocity. Subsequently, when the waves have attained their maximum amplitude the sheet tends to break down at the crests and troughs into half-wavelengths. In the present case, waves covering a range of sizes are superimposed on the sheets. Since a sheet will break down only when the waves have grown to a critical amplitude, the resulting sheet fragments may contain a varying number of wavelengths. There is, however, an important similarity between 'impact' and aerodynamic-wave disintegration. In each case both the wavelengths and break-up distance decreases with increase of jet velocity. Since the rate of increase of sheet thickness at break-up is less than the corresponding rate of decrease in wavelength the resulting drop size diminishes with increase of velocity.

Figure 4 demonstrates that, for sheets produced by laminar jet impingement, the process of drop formation varies with impact velocity. Thus for example, at an angle of 110° and a velocity of 730 cm/sec, a stationary thick rim is produced from which relatively coarse drops are produced. At a velocity of 1160 cm/sec impact waves are generated. Although these waves are soon damped, disturbances persist along the extent of the sheet and prevent the formation of the thick rim. Under these conditions the sheet still breaks down some distance away from the origin and since its thickness is relatively small at this point, smaller drops are produced. When the velocity is increased to 1950 cm/sec, impact wave disintegration predominates and the sheet breaks up very close to the origin where it is fairly thick. The corresponding wavelength results in a drop size greater than that at 1160 cm/sec. Impact-wave disintegration appears to be established at 1950 cm/sec and it is likely that the drop size will tend to diminish at higher jet velocities in a manner similar to that found for turbulent jet impingement.

The authors are indebted to Mr R. P. Fraser and Dr P. Eisenklam for valuable advice.

REFERENCES

DOMBROWSKI, N. & FRASER, R. P. 1954 *Phil. Trans.* A, **247**, 101.
DOMBROWSKI, N. & HOOPER, P. C. 1962 *Fuel*, **41**, 323.
FRY, F. J., THOMAS, P. H. & SMART, P. M. 1954 *Quart. Inst. Fire Engrs, Edinb.* **14**, 4.
HEIDMAN, M. F., PRIEM, R. J. & HUMPHREY, J. C. 1957 *N.A.C.A. Tech. Note*, no. 3835.
HOOPER, P. C. 1959 Ph.D. Thesis, London University.
RUPE, J. H. 1953 *Jet Prop. Lab. C.I.T. Progr. Rep.* 20-299.
STEHLING, K. R. 1952 *J. Amer. Rocket Soc.* **22**, 132.
TANASAWA, Y., SASAKI, S. & NAGAI, N. 1957 *Tech. Rep. Tohoku University*, **22**, 73.
TAYLOR, G. I. 1960 *Proc. Roy. Soc.* A, **259**, 1.

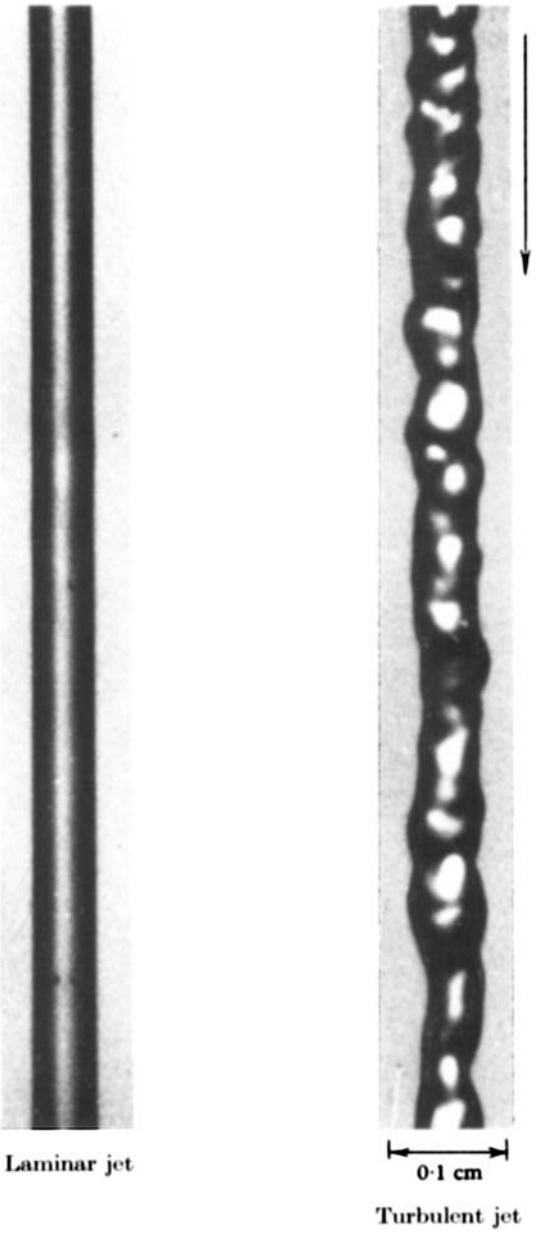

FIGURE 1. Photographs of jets 0·16 cm from orifice.

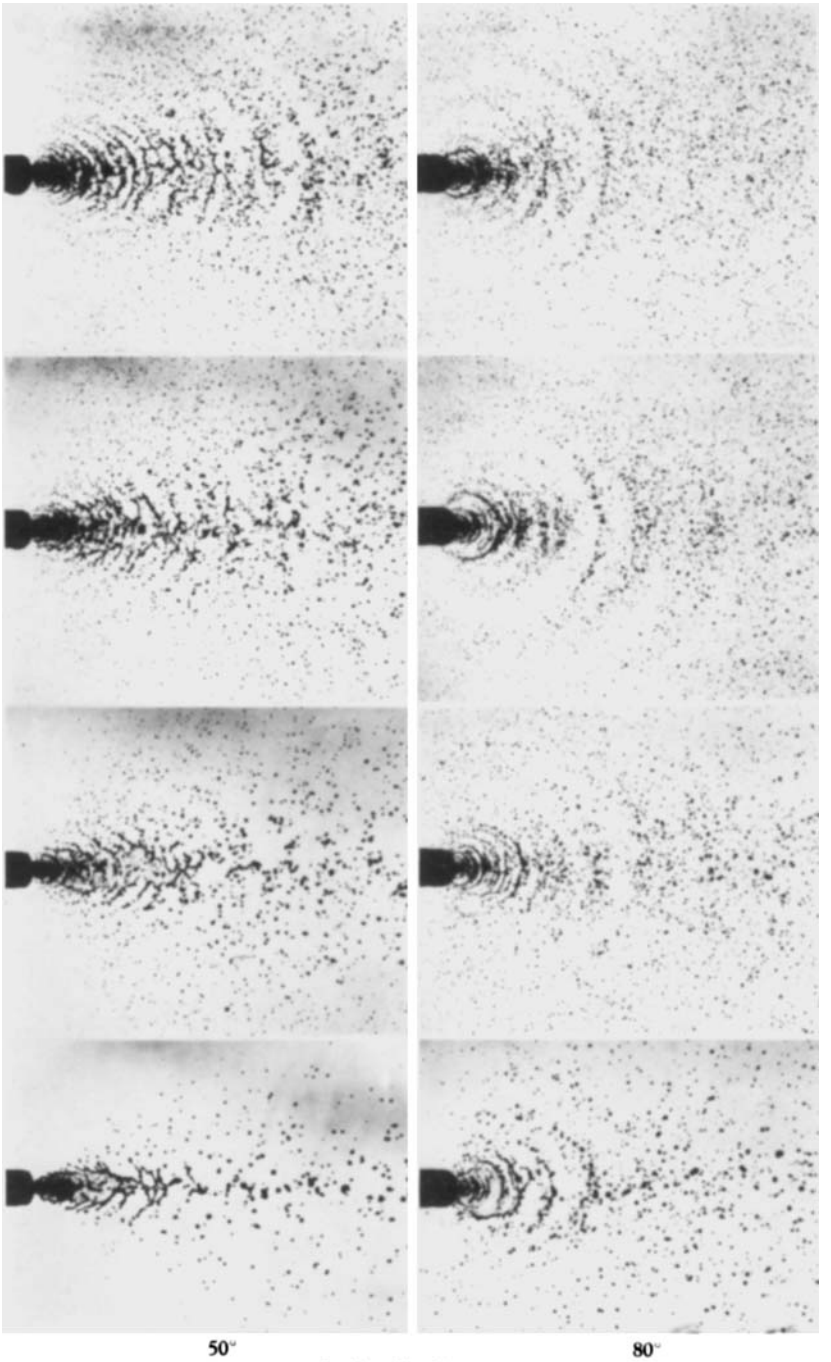

Angle of impingement

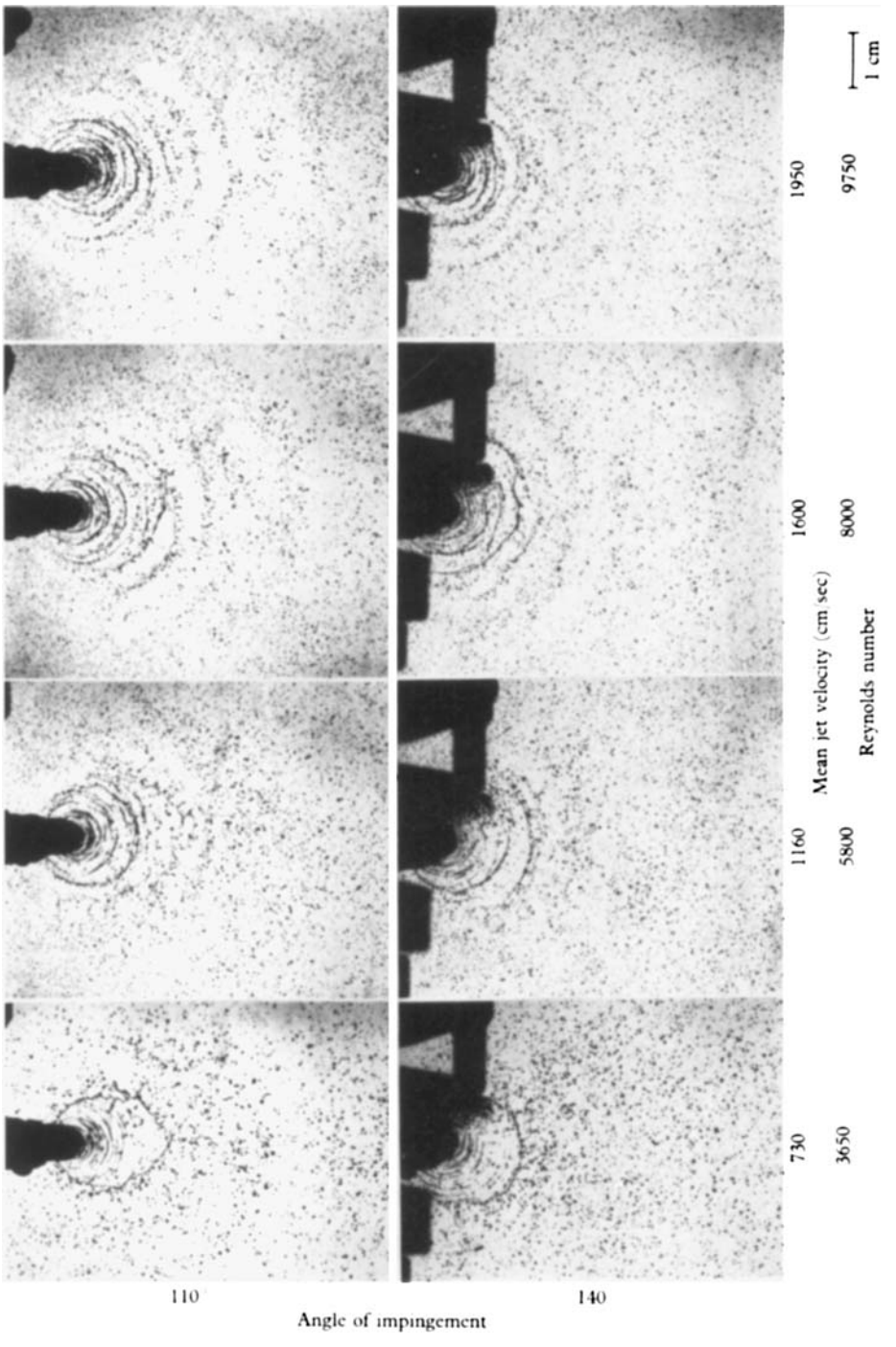

FIGURE 3. Impingement of turbulent jets.

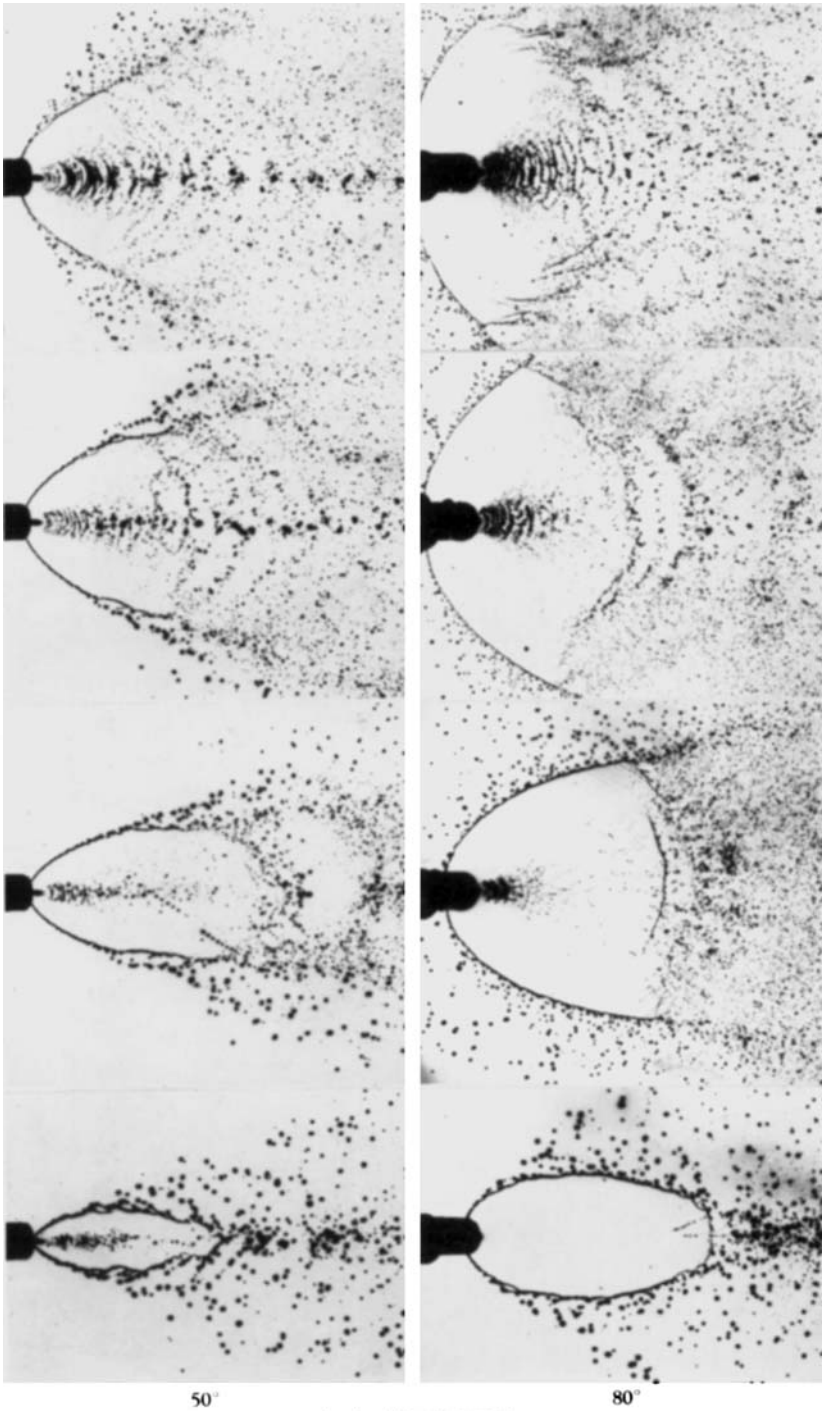

Angle of impingement

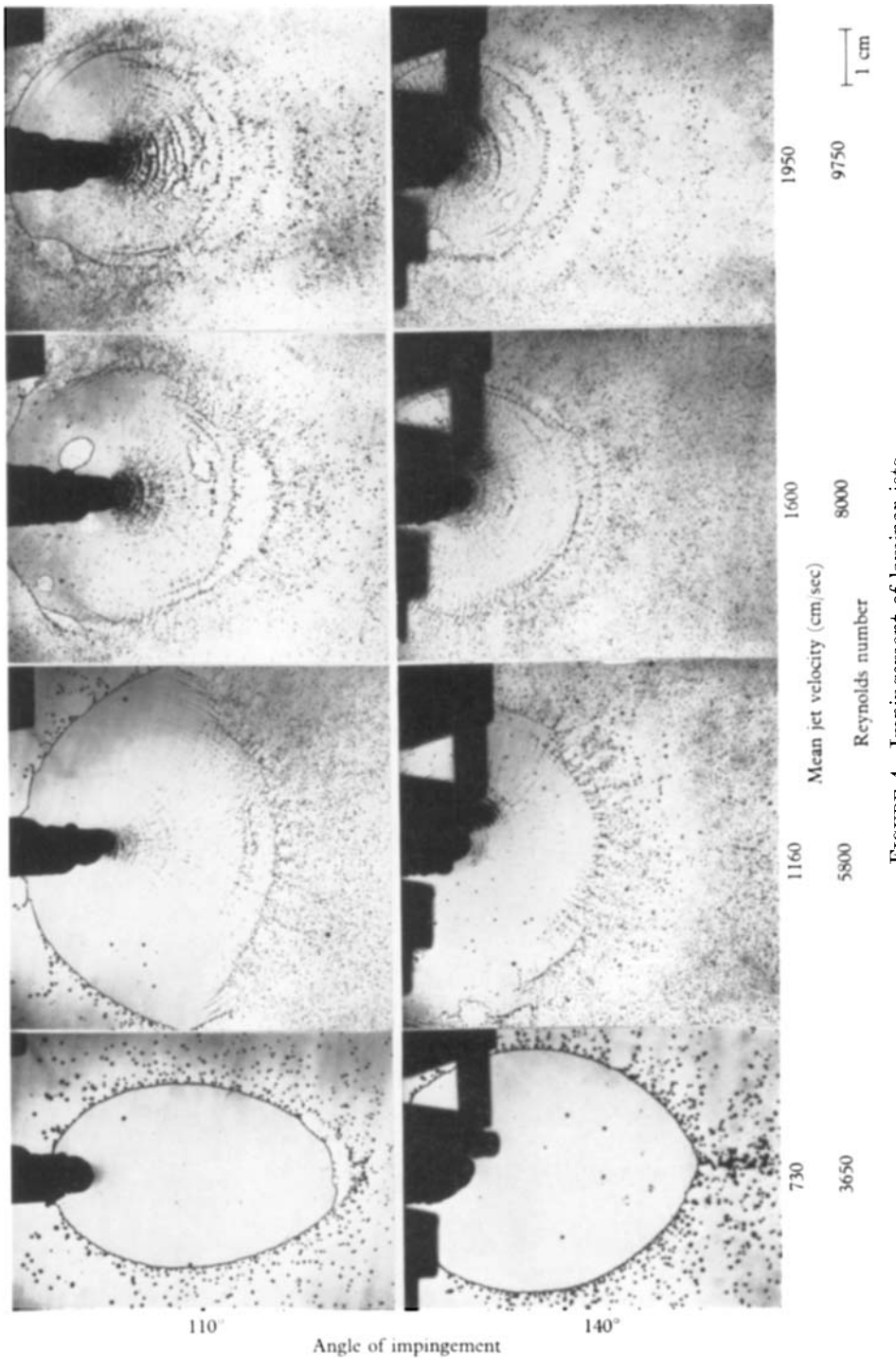

FIGURE 4. Impingement of laminar jets.

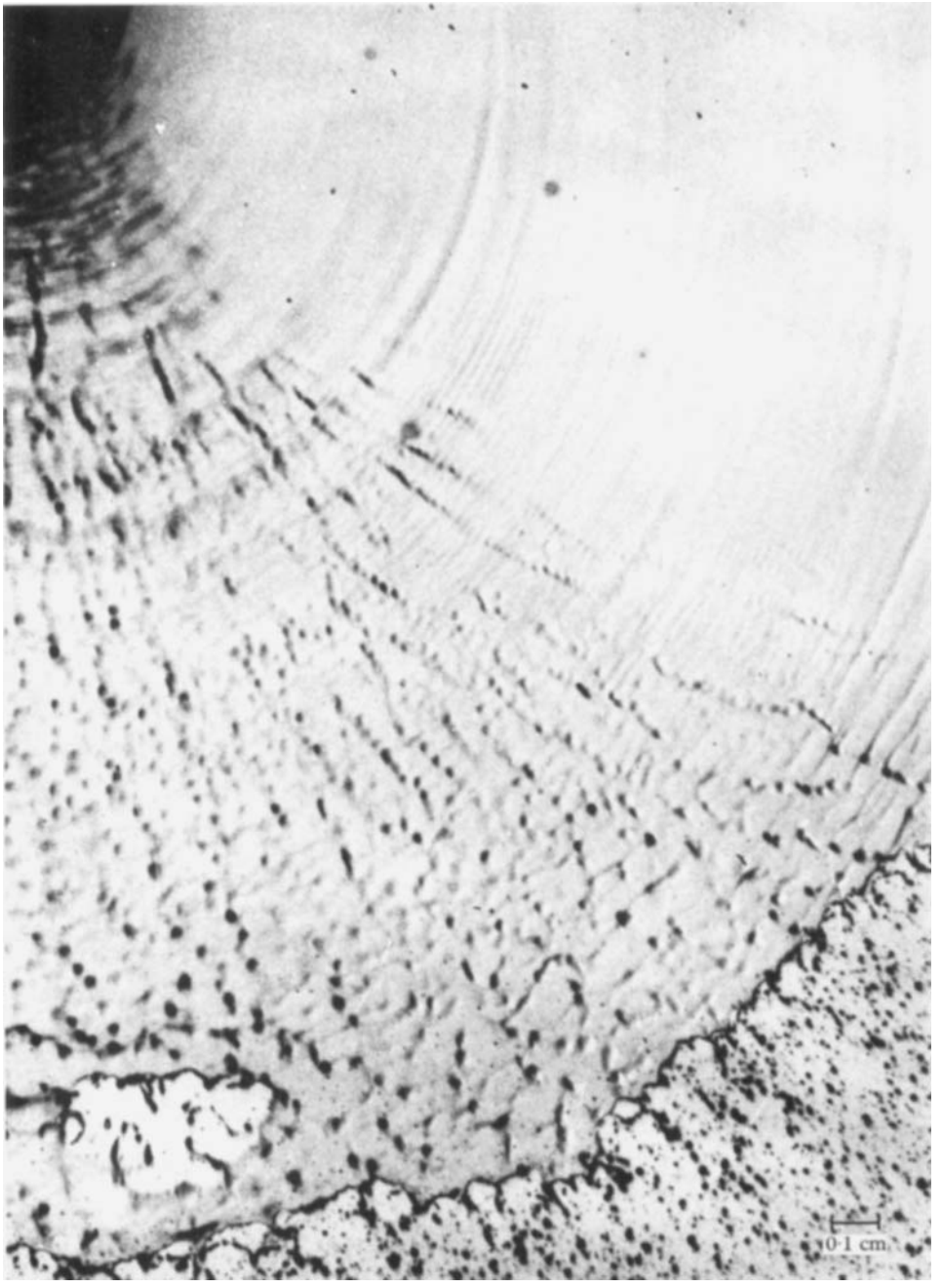

FIGURE 5. Impingement of laminar jets.